

# Parametrically excited systems and applications on the dynamics of slender structures

PEF 6000 - Special topics on dynamics of structures

**Associate Professor Guilherme R. Franzini**  
**PhD Candidate Guilherme J. Vernizzi**

- 1 Objectives and references
- 2 General definitions
- 3 Strutt's diagram
- 4 Horizontal cable
- 5 Dynamics of slender and straight offshore structures vertically hanged
- 6 Floquet theory - introduction
- 7 Use of the harmonic balance method (HBM)



# Outline

- 1 Objectives and references
- 2 General definitions
- 3 Strutt's diagram
- 4 Horizontal cable
- 5 Dynamics of slender and straight offshore structures vertically hanged
- 6 Floquet theory - introduction
- 7 Use of the harmonic balance method (HBM)

- To introduce to basic aspects related parametrically excited systems;
- Focuses of the classes: Importance on cable dynamics, evaluation of stability maps (Strutt's diagram), introduction to Floquet theory;
- Examples of references
  - ① Nayfeh, A.H. 1973. *Perturbation methods*. John Wiley & Sons.
  - ② Nayfeh, A.H. & Mook, D.T. 1979. *Nonlinear oscillations*. John Wiley & Sons.
  - ③ Nayfeh, A.H. & Balachandran, B. 1995. *Applied Nonlinear Dynamics - Analytical, Computational and Experimental Methods*. John Wiley & Sons.
  - ④ Franzini, G.R. 2019. *Tópicos de pesquisa em problemas de excitação paramétrica e de vibrações induzidas pelo escoamento*. Habilitation thesis. Escola Politécnica da Universidade de São Paulo.
  - ⑤ Selected papers.

# Outline

- 1 Objectives and references
- 2 General definitions**
- 3 Strutt's diagram
- 4 Horizontal cable
- 5 Dynamics of slender and straight offshore structures vertically hanged
- 6 Floquet theory - introduction
- 7 Use of the harmonic balance method (HBM)

# General definitions

- A system is non-autonomous if its dynamics is governed by a system of first-order ODEs given by  $\dot{x}_i = f_i(\mathbf{x}, t, \boldsymbol{\mu})$ ,  $\boldsymbol{\mu}$  being a vector with the parameters of the mathematical model. On the other hand, an autonomous system is given by  $\dot{x}_i = f_i(\mathbf{x}, \boldsymbol{\mu})$
- The explicit dependence on time arises either from an external excitation (for example, an external harmonic load) or from a (or more than one) parameter that varies with respect to time. The focus herein is on problems in which the stiffness harmonically varies with respect to time;
- Problems in which one or more parameters of the mathematical model explicitly depend on time are called parametrically excited systems.

# General definitions

- Hill's equation  $\rightarrow \ddot{u} + p(t)u = 0$ ,  $p(t)$  a periodic function;
- Mathieu's equation  $\rightarrow \ddot{u} + (\delta + 2\epsilon \cos 2t)u = 0$ ;
- If these equations represent the dynamics of a mechanical system, the stiffness explicitly depends on time ( $k = k(t)$ );
- **Both are linear equations.**



# Outline

- 1 Objectives and references
- 2 General definitions
- 3 Strutt's diagram**
- 4 Horizontal cable
- 5 Dynamics of slender and straight offshore structures vertically hanged
- 6 Floquet theory - introduction
- 7 Use of the harmonic balance method (HBM)

- Indicates the regions of the plane of control parameters  $(\epsilon; \delta)$  associated with bounded or unbounded responses. **We will obtain the transition curves using the Floquet theory and the harmonic balance method.**
- We will see that the transition curves correspond to periodic solutions of period  $T$  or  $2T$ .

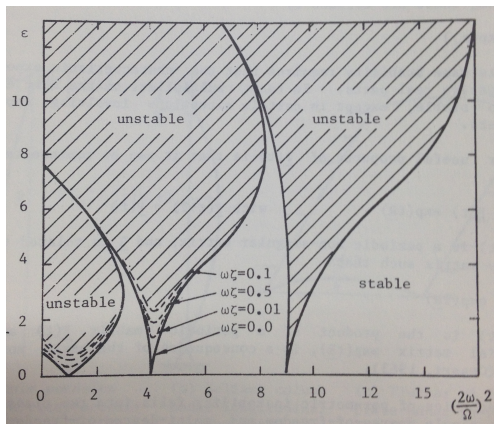


Figure: Extracted from Ibrahim (2007).

Obs: Figure above corresponds to the Strutt's diagram for  
 $\ddot{x} + 2\zeta\omega\dot{x} + (\omega^2 - 2\epsilon \cos \Omega t)x = 0$ .



# Outline

- 1 Objectives and references
- 2 General definitions
- 3 Strutt's diagram
- 4 Horizontal cable**
- 5 Dynamics of slender and straight offshore structures vertically hanged
- 6 Floquet theory - introduction
- 7 Use of the harmonic balance method (HBM)

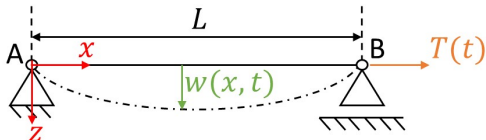


Figure: Horizontal cable under parametric excitation.

- As already showed, the equation of motion of a horizontal cable is given by

$$\mu \ddot{w} - T(t) w'' = 0 \quad (1)$$

- Solutions with the form  $w(x, t) = \psi_n(x)A_n(t)$  (separation of variables) are sought. By substituting this expression into the equation of motion, we obtain:

$$\mu\psi_n(x)\ddot{A}_n(t) - T(t)\psi_n''(x)A_n(t) = 0 \quad (2)$$

# Formulation

- Using the Galerkin's method:

$$\int_0^L \mu \psi_n^2(x) dx \ddot{A}_n - \int_0^L T(t) \psi_n(x) \psi_n''(x) dx A_n = 0 \quad (3)$$

- By adopting the natural modes of vibration of the horizontal cable,  $\psi_n(x) = \sin\left(\frac{n\pi}{L}x\right)$ ,  $n = 1, 2, 3 \dots$ , we obtain:

$$\int_0^L \mu \psi_n^2(x) dx = \frac{\mu L}{2} = m; \quad (4)$$

$$- \int_0^L T(t) \psi_n(x) \psi_n''(x) dx = \frac{n^2 \pi^2}{2L} T(t) = k(t) \quad (5)$$

$$m \ddot{A}_n + k(t) A_n(t) = 0 \quad (6)$$

- Hint: when using a numerically obtained function for  $\psi_n(x)$  it is possible to achieve better accuracy by using integration by parts to work with the smaller order possible for derivatives.

## Formulation

- We assume that the tension varies as  $T(t) = \bar{T} + \Delta T \cos \Omega t$ ,  $\Delta T < \bar{T}$

$$k(t) = \frac{n^2 \pi^2}{2L} \bar{T} + \frac{n^2 \pi^2}{2L} \Delta T \cos \Omega t \quad (7)$$

- For the sake of generality, we rewrite the ODE in the corresponding dimensionless form. For this, we define  $\tau = \frac{1}{2} \Omega t$  as the dimensionless time. The derivatives with respect to the dimensional time read:

$$(\dot{\phantom{x}}) = \frac{\Omega}{2} \frac{d}{d\tau}(\phantom{x}), (\ddot{\phantom{x}}) = \frac{\Omega^2}{4} \frac{d^2}{d\tau^2}(\phantom{x}) \quad (8)$$

- Using these quantities in the 1-dof ROM, we obtain:

$$\frac{d^2 A(\tau)}{d\tau^2} + \left( \left( \frac{2n\pi}{\Omega L} \right)^2 \frac{\bar{T}}{\mu} + \left( \frac{2n\pi}{\Omega L} \right)^2 \frac{\Delta T}{\mu} \cos(2\tau) \right) A(\tau) = 0 \quad (9)$$

$$\frac{d^2 A(\tau)}{d\tau^2} + (\delta + 2\epsilon \cos 2\tau) A(\tau) = 0 \quad (10)$$

- Conclusion: Cables subjected to time-dependent normal force (tension) are parametrically excited;
- Obs: If we adopt another dimensionless time, the Mathieu's equation will be given in a different form.

# Parametric instability

- Two parameters govern the parametric excitation, namely, its amplitude and frequency. In the Mathieu's equation herein discussed, these parameters are, respectively,  $\epsilon$  e  $\delta$ .
- Depending on the values of  $\epsilon$  e  $\delta$ , the trivial solution loss stability and unbounded responses appear. This phenomenon is known as parametric instability (or Mathieu's instability).



# Outline

- 1 Objectives and references
- 2 General definitions
- 3 Strutt's diagram
- 4 Horizontal cable
- 5 Dynamics of slender and straight offshore structures vertically hanged**
- 6 Floquet theory - introduction
- 7 Use of the harmonic balance method (HBM)

- *Risers*. Slender and tubular structures, used to convey gas and oil from the seabed to a floating unit;
- TLPs - *Tension leg platforms*. A type of floating unit consisted of a platform kept in place by the use of vertical tethers fixed to the seabed;
- Nonlinear effects may be important in the dynamic behavior of TLP tethers and *risers* due to their slenderness.

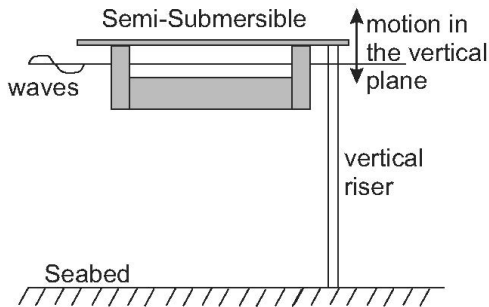


Figure: Extracted from Franzini et al (2014).

The tension along the riser depends explicitly on time due to the vertical motion of the floating unit.

## Examples of references

- Rainey (1977): One of the first works in the field, focused on the dynamics of TLPs.
- Patel & Park (1991): Studies the Strutt diagram for the tethers of a TLP for large values of  $\delta$  and  $\varepsilon$ . The effect of the the hydrodynamic damping is also considered.  $\rightarrow$  The nonlinear hydrodynamic damping in the form  $\beta|\dot{x}|\dot{x}$  limits the amplitudes of motion even in the unstable regions of Strutt's diagram. **The linearization of the damping eliminates this important property for the dynamic behavior of the structure.**
- Simos & Pesce (1997): Takes into account the effects of the distributed load due to the structural weight on the Strutt's diagram for the problem.

## Examples of references

- Franzini et al (2016): Study of the influence of hydrodynamic coefficients (additional mass and drag coefficient) on the amplitude of steady-state motion;
- Mazzilli et al (2014): Brings a mathematical deduction for the nonlinear modes of vibration of a vertical beam under self-weight load. The formulation also allows to obtain the “Bessel-Like” functions that represents a very good approximation for the shape of the linear modes of vibration of this type of structure;
- Mazzilli & Dias (2014): Presents a reduced order model with a single degree of freedom by means of a “Bessel-Like” function.

- Analysis of an experiment made with an immerse and flexible structure;
- Harmonic motions were imposed to the top of the structure with a constant amplitude  $A_t/L_0 = 1\%$  and different frequencies;
- The displacements were monitored in various points along the structure by means of an optical tracking system;
- The experiment is part of a comprehensive project on nonlinear dynamics of risers made by the research group during the years between 2009 and 2013.

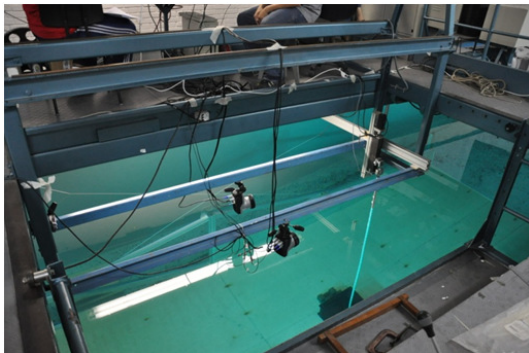


Figure: Extracted from Franzini et al (2015).



Figure: Extracted from Franzini et al (2015).

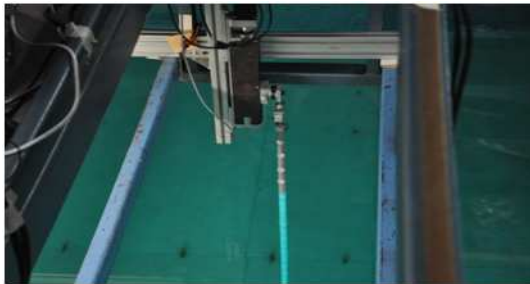


Figure: Extracted from Franzini et al (2015).

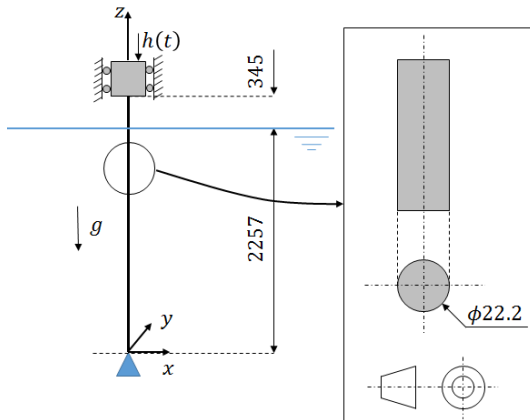


Figure: Extracted from Franzini et al (2015).

Table: Nondimensional parameters. Extracted from Rateiro et al (2012).

Number	Symbol	Representation
Froude number	$F_r = \frac{\omega A}{\sqrt{gL}}$	Dynamic motion in waves
Reynolds number	$Re = \frac{UD}{\nu}$	Inertial forces vs viscous forces
Strouhal number	$St = \frac{f_s D}{U}$	Vortex shedding frequency
Keulegan-Carpenter number	$KC = \frac{2\pi A}{D}$	Inertial forces vs drag forces
Structural damping	$\zeta = \frac{c}{c_c}$	Linear structural damping
Reduced velocity	$V_R = \frac{U}{f_n D}$	Normalized velocity in VIV
Reduced shedding frequency	$f_s^* = \frac{f_s}{f_n} = S_t \frac{U}{f_n D} = S_t V_R$	Vortex shedding normalized frequency
Reduced mass	$m^* = \frac{m}{m_D}$	Riser mass vs displaced mass
Added mass	$a = \frac{m_a}{m}$	Added mass vs riser mass
Bending stiffness	$K_f = \frac{\lambda f}{L}$	Bending vs. geometrical stiffness
Axial stiffness	$K_a = \frac{EA}{T}$	Axial vs. geometrical stiffness

Table: Complementary model properties.

Property	Value
Internal diameter	15.8 mm
External diameter $D$	22.2 mm
Unstretched length $L_o$	2552 mm
Stretched length $L$	2602 mm
Immersed length $L_i$	2257 mm
Immersed weight $\gamma$	7.88 N/m
Axial stiffness $EA$	1.2 kN
Bending stiffness $EI$	0.056 N m <sup>2</sup>
Mass ratio parameter $m^*$	3.48
Aspect ratio $L_i/D$	102
$L/D$	117
Static tension at the top $T_t$	40 N

- Idea applied to the analysis: The Galerkin method was applied to the time series of the model in order to obtain “modal Strutt diagrams”. The modal amplitude of mode  $n$  is given by:

$$u_n(t) = \frac{\langle x(z, t), \psi_n(z) \rangle}{\langle \psi_n(z), \psi_n(z) \rangle} = \frac{\int_0^L x(z, t) \psi_n(z, t) dz}{\int_0^L \psi_n^2(z, t) dz} \quad (11)$$

- Sine functions were used in the Galerkin method:  $\psi_n(z) = \sin(n\pi z/L_0)$

Reconstruction of an instantaneous deformed configuration:

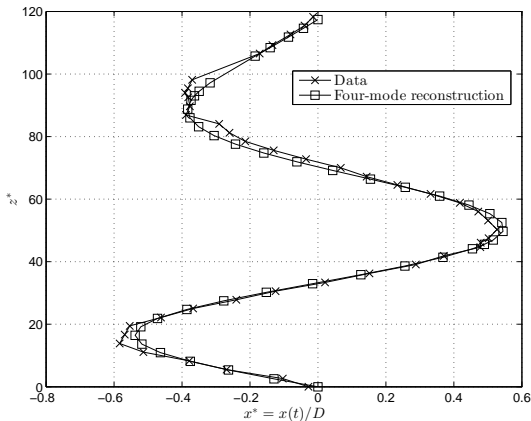


Figure: Extracted from Franzini et al (2015).  $f_t : f_{N,1} = 3 : 1$ .

Free vibrations test - decay:

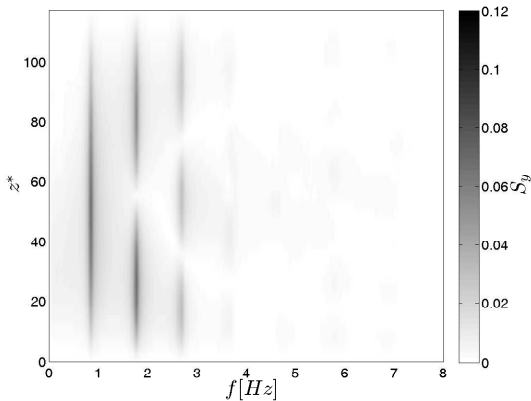


Figure: Extracted from Franzini et al (2015).

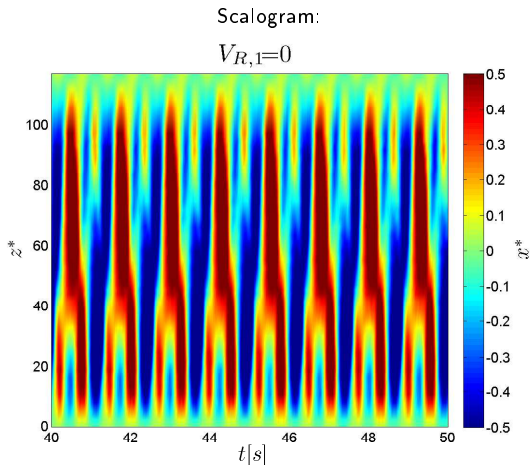


Figure: Extracted from Franzini et al (2015).  $f_t : f_{N,1} = 2 : 1$ .

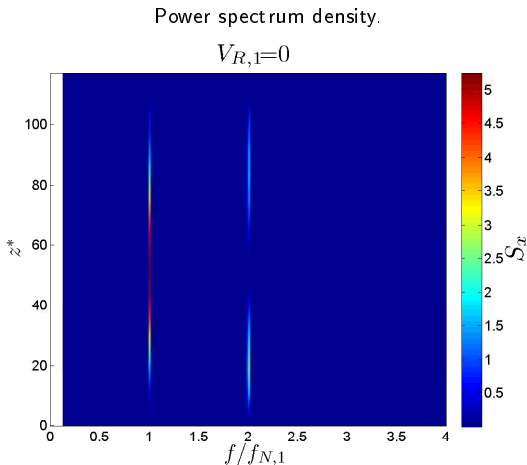


Figure: Extracted from Franzini et al (2015).  $f_t : f_{N,1} = 2 : 1$ .

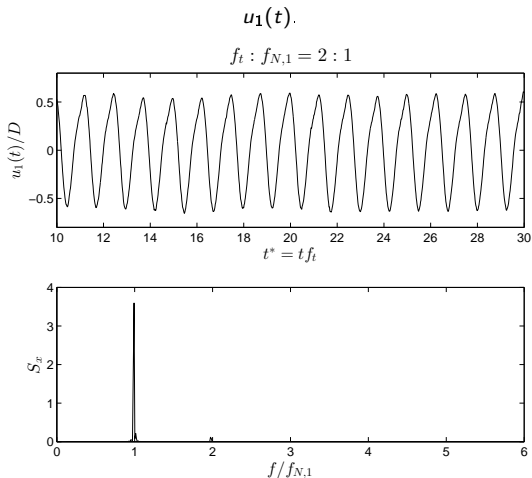


Figure: Extracted from Franzini et al (2015).  $f_t : f_{N,1} = 2 : 1$ .

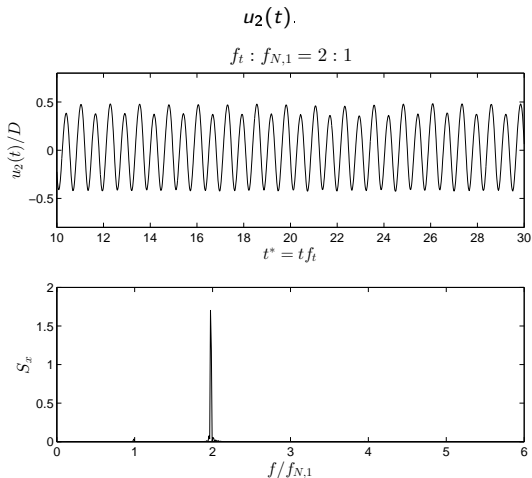


Figure: Extracted from Franzini et al (2015).  $f_t : f_{N,1} = 2 : 1$ .

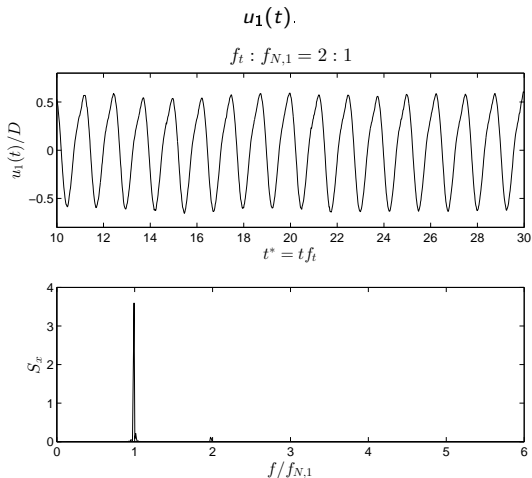


Figure: Extracted from de Franzini et al (2015).  $f_t : f_{N,1} = 1 : 1$ .

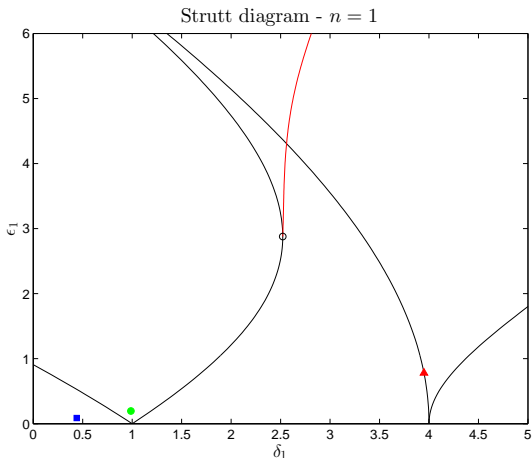


Figure: Extracted from Franzini et al (2015). Red:  $f_t : f_{N,1} = 1 : 1$ , green:  $f_t : f_{N,1} = 2 : 1$ , blue:  $f_t : f_{N,1} = 3 : 1$ .

- Starting point: Nonlinear equation of motion of a tensioned vertical beam (disregarding the axial dynamics).

$$\begin{aligned}
 & m_I \frac{\partial^2 u}{\partial t^2} + c \frac{\partial u}{\partial t} + EI \frac{\partial^4 u}{\partial z^4} - \frac{\partial}{\partial z} \left( T(t, z) \frac{\partial u}{\partial z} \right) \\
 & - \frac{EA}{2L_0} \frac{\partial^2 u}{\partial z^2} \int_0^{L_0} \left( \frac{\partial u}{\partial z} \right)^2 dz \\
 & = -m_a \frac{\partial^2 u}{\partial t^2} - \frac{1}{2} \rho D \overline{C_D} \left| \frac{\partial u}{\partial t} \right| \frac{\partial u}{\partial t}
 \end{aligned} \tag{12}$$

Hydrodynamic forces: Potential added mass (Forcing term with the same phase of the cross-section acceleration); Viscous damping (Quadratic with the relative speed between fluid and structure - Morison damping).

- Product derivative identity:

$$\gamma \frac{\partial u}{\partial z} + T(z) \frac{\partial^2 u}{\partial z^2} = \frac{\partial}{\partial z} \left( T(t, z) \frac{\partial u}{\partial z} \right) \quad (13)$$

- Tension along the structure:

$$T(t, z) = \bar{T}_t - \gamma(L_0 - z) + \frac{EA}{L_0} A_t \cos(\Omega t) \quad (14)$$

- Multi-mode solution:

$$u(z, t) = \sum_{k=1}^3 \psi_k(z) A_k(t) \quad (15)$$

- Useful dimensionless quantities:

$$\begin{aligned} \tau &= t\omega_1; n = \frac{\Omega}{\omega_1}; \hat{A}_k = A_k/D; \\ C_a &= \frac{m_a}{m_d}; \tilde{m} = \frac{m_l}{m_d}; \Lambda_M = \frac{D^2}{L_0 m_d (\tilde{m} + C_a)} \rho \overline{C_D} \end{aligned} \quad (16)$$

Equation for  $n = 1$

$$\begin{aligned}
 & \frac{d^2 \hat{A}_1}{d\tau^2} + \alpha_1 \frac{d\hat{A}_1}{d\tau} + (\delta_1 + \epsilon_1 \cos(n\tau)) \hat{A}_1 + \alpha_2 \hat{A}_2 + \alpha_3 \hat{A}_1^3 + \\
 & \alpha_4 \hat{A}_2^2 \hat{A}_1 + \alpha_5 \hat{A}_1 \hat{A}_3^2 + \\
 & \Lambda_M \int_0^{L_0} \left| \sum_{n=0}^3 \frac{d\hat{A}_n}{d\tau} \psi_n \right| \left( \sum_{n=0}^3 \frac{d\hat{A}_n}{d\tau} \psi_n \right) \psi_1 dz = 0
 \end{aligned}
 \tag{17}$$

Equation for  $n = 2$

$$\begin{aligned}
 & \frac{d^2 \hat{A}_2}{d\tau^2} + \beta_1 \frac{d\hat{A}_2}{d\tau} + (\delta_2 + \epsilon_2 \cos(n\tau))\hat{A}_2 + \beta_2 \hat{A}_3 + \beta_3 \hat{A}_1 + \\
 & \beta_4 \hat{A}_2 \hat{A}_1^2 + \beta_5 \hat{A}_2^3 + \beta_6 \hat{A}_2 \hat{A}_3^2 + \\
 & \Lambda_M \int_0^{L_0} \left| \sum_{n=0}^3 \frac{d\hat{A}_n}{d\tau} \psi_n \right| \left( \sum_{n=0}^3 \frac{d\hat{A}_n}{d\tau} \psi_n \right) \psi_2 dz = 0
 \end{aligned} \tag{18}$$

Equation for  $n = 3$

$$\begin{aligned}
 & \frac{d^2 \hat{A}_3}{d\tau^2} + \gamma_1 \frac{d\hat{A}_3}{d\tau} + (\delta_3 + \epsilon_3 \cos(n\tau)) \hat{A}_3 + \gamma_2 \hat{A}_2 + \gamma_3 \hat{A}_3 \hat{A}_2^2 + \\
 & \gamma_4 \hat{A}_3 \hat{A}_1^2 + \gamma_5 \hat{A}_3^3 + \\
 & \Lambda_M \int_0^{L_0} \left| \sum_{n=0}^3 \frac{d\hat{A}_n}{d\tau} \psi_n \right| \left( \sum_{n=0}^3 \frac{d\hat{A}_n}{d\tau} \psi_n \right) \psi_3 dz = 0
 \end{aligned} \tag{19}$$

- The equations for the three vibration modes were numerically integrated (using the Runge-Kutta method) and the modal amplitudes in steady-state regime were obtained for various pairs of amplitude/frequency of the parametric excitation.

Example of result:

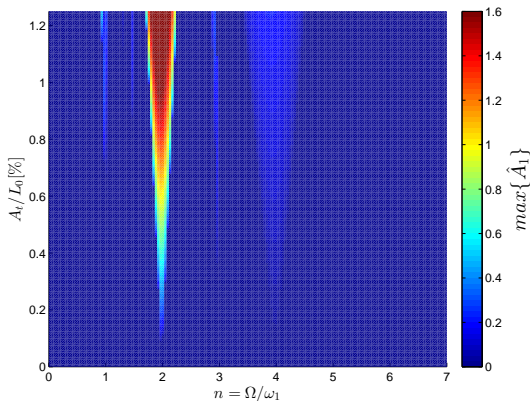


Figure: Extracted from Franzini & Mazzilli (2016).

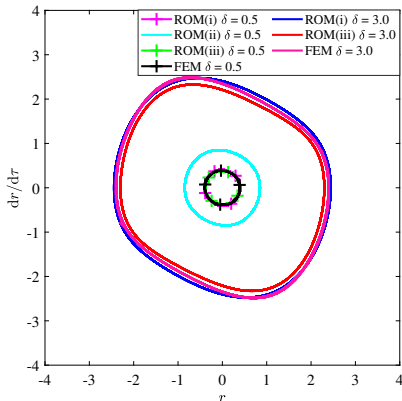
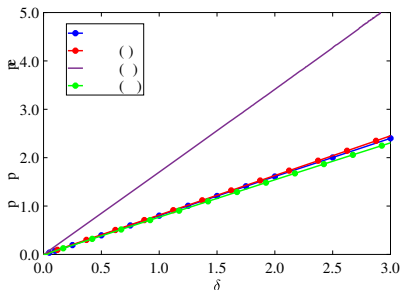
- Starting point: Nonlinear equation of motion of a tensioned vertical beam (disregarding the axial dynamics);
- Focus: Comparison of the use of different projection functions when using the Galerkin's method to obtain reduced order models (ROMs);
- Models considered:
  - ROM(i): a single “Bessel-like” function in the projection;
  - ROM(ii): a single Sine function in the projection;
  - ROM(iii): three Sine functions in the projection (Franzini & Mazzilli (2016));
- Main conclusion: “better” projection functions (closer to the actual modes of vibration) allows the use of a smaller ROM, which in turn allows the straightforward use of analytical techniques.

- Dimensionless equation for a ROM with a single degree of freedom:

$$\frac{d^2 r}{d\tau^2} + \beta_1 \frac{dr}{d\tau} + (1 + \beta_2 \delta \cos(n\tau)) r + \beta_3 r^3 + \beta_4 \left| \frac{dr}{d\tau} \right| \frac{dr}{d\tau} = 0 \quad (20)$$

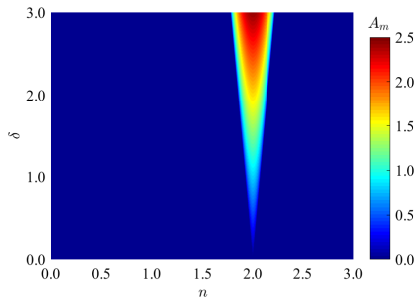
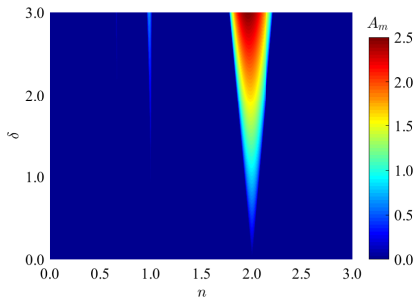
- $r$  is the dimensionless displacement,  $\tau$  the dimensionless time,  $\beta$  are parameters depending on the Galerkin integrals and the parametric excitation is ruled by the parameters  $\delta$  and  $n$ .
- Using the method of multiple scales and expanding the absolute value function in Fourier series is possible to obtain an algebraic expression for the steady-state amplitude.

Comparison between ROMs and Finite Element solutions:



Extracted from Vernizzi et al (2019).

Comparison between analytical solution and numerical integration for ROM(i):



Extracted from Vernizzi et al (2019).

Computational advantage:

Table: Comparison of computational time required by each type of solution.

Model	Method	Simulation of a $600 \times 600$ map (s)	Single simulation (s)
FEM	Numerical	—	$1.342 \times 10^3$
ROM(i)	Numerical	$29.3 \times 10^3$	0.082
ROM(i)	Analytical	$11.5 \times 10^{-3}$	$3.194 \times 10^{-8}$
ROM(iii)	Numerical	$114.9 \times 10^3$	0.319

Extracted from Vernizzi et al (2019).

The analytical solution allows an easy and fast investigation of the structure, being an useful tool to aid the evaluation of the influence of changing some parameters such as cross-section dimensions or material.

- Starting point: Nonlinear equation of motion of a tensioned vertical beam with axial dynamics;
- Axial equation:

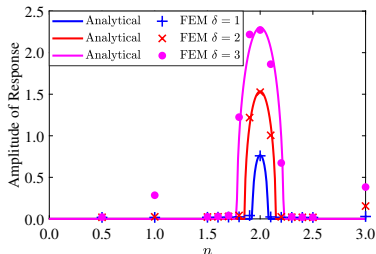
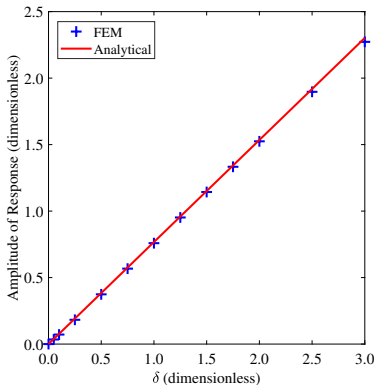
$$\mu \ddot{W} + c_a \dot{W} + \gamma - EA (W'' + V' V'') = 0 \quad (21)$$

- Transversal equation:

$$\begin{aligned}
 & (\mu + \mu_a) \ddot{V} + c \dot{V} + \frac{1}{2} \rho D \overline{C_D} |\dot{V}| \dot{V} + EIV'''' \\
 & - EA \left( W'' V' + W' V'' + \frac{3}{2} (V')^2 V'' \right) = 0 \quad (22)
 \end{aligned}$$

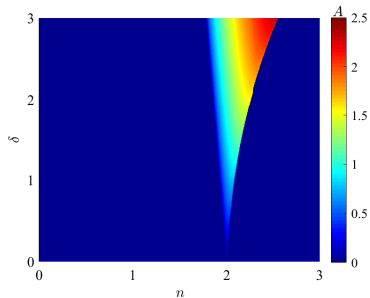
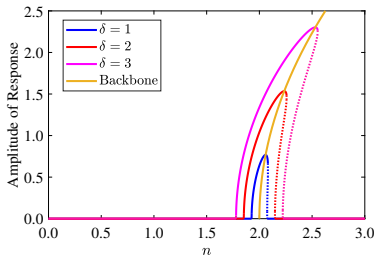
- The solution is sought with the application of the method of multiple scales directly on the partial differential equations;
- Motivation: In some problems the Galerkin method may lead to qualitative errors in the behavior of the dynamic system (Book “Nonlinear Stability and Bifurcation Theory: An Introduction for Engineers and Applied Scientists”, Hans Troger & Alois Steindl, 1991). **Question not yet fully answered: What are the properties of a dynamical system that guarantees the success or failure of Galerkin's method.**
- Studies of the influence of nonlinear stiffness and damping effects are also carried out in the paper.

Comparison between analytical and Finite Element solutions:



Extracted from Vernizzi et al (2020).

Example of parameter investigation:



Extracted from Vernizzi et al (2020).

Example of parameter investigation:

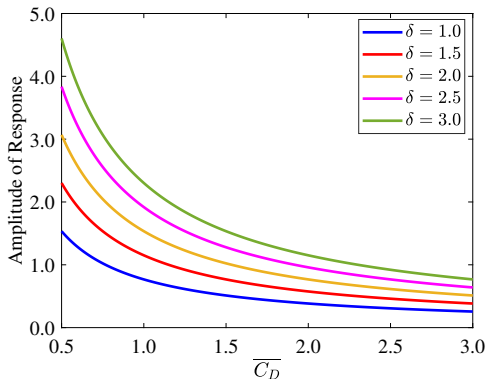


Figure: Extracted from Vernizzi et al (2020).

# Outline

- 1 Objectives and references
- 2 General definitions
- 3 Strutt's diagram
- 4 Horizontal cable
- 5 Dynamics of slender and straight offshore structures vertically hanged
- 6 Floquet theory - introduction**
- 7 Use of the harmonic balance method (HBM)

- Floquet theory: Useful for the stability analysis of periodic orbits;
- Focus of this class: Application to the Mathieu's equation;
- Consider the following equation, with  $p_1(t)$  and  $p_2(t)$  periodic functions of period  $T$  ( $p_1(t) = p_1(t + T)$  and  $p_2(t) = p_2(t + T)$ );

$$\ddot{u} + p_1(t)\dot{u} + p_2(t)u = 0 \quad (23)$$

- We can use the change of variables  $u = xe^{-\frac{1}{2} \int p_1(\tau) d\tau}$  in Eq. 23 to obtain the Hill's equation (Eq. 24)

$$\ddot{x} + p(t)x = 0 \quad (24)$$

$$p(t) = p_2(t) - \frac{p_1^2(t)}{4} - \frac{\dot{p}_1(t)}{2} \quad (25)$$

- Since Eq. 23 is linear, its solution is given in the general form  $u(t) = c_1 u_1(t) + c_2 u_2(t)$ ,  $u_1(t)$  and  $u_2(t)$  being two fundamental solutions of Eq. 23.

- We show that  $u_1(t + T)$  (and, analogously,  $u_2(t + T)$ ) is also a solution of Eq. 23:

$$\ddot{u}_1(t + T) + \underbrace{p_1(t)}_{p_1(t+T)} \dot{u}_1(t + T) + \underbrace{p_2(t)}_{p_2(t+T)} u_1(t + T) = 0 \quad (26)$$

- Since  $u_1(t + T)$  and  $u_2(t + T)$  are solutions of Eq. 23, they are written as linear combinations of  $u_1(t)$  and  $u_2(t)$  as

$$u_1(t + T) = a_{11}u_1(t) + a_{12}u_2(t) \quad (27)$$

$$u_2(t + T) = a_{21}u_1(t) + a_{22}u_2(t) \quad (28)$$

- Defining  $\mathbf{u}(t) = \{u_1(t + T) \ u_2(t + T)\}^T$ , we have  $\mathbf{u}(t + T) = \mathbf{A}\mathbf{u}(t)$ , with  $\det(\mathbf{A}) \neq 0$ .

- Let  $\mathbf{v}(t)$  being another set of fundamental solutions. In this case,  $\mathbf{v}(t)$  is also a linear combination of the elements of  $\mathbf{u}(t)$ ;

$$\begin{aligned}\mathbf{u}(t) = P\mathbf{v}(t) &\rightarrow \mathbf{u}(t + T) = P\mathbf{v}(t + T) = \mathbf{A}\mathbf{u}(t) \leftrightarrow \\ \leftrightarrow \mathbf{v}(t + T) &= P^{-1}\mathbf{A}\mathbf{u}(t) = \underbrace{P^{-1}\mathbf{A}P}_{\mathbf{B}}\mathbf{v}(t)\end{aligned}\quad (29)$$

- It can be proved that  $\mathbf{A}$  and  $\mathbf{B}$  have the same eigenvalues;
- We conveniently choose  $P$  for obtaining  $\mathbf{B}$  in a Jordan's form.

## Case i - $B$ has distinct eigenvalues

- In this case, we have:

$$B = \begin{bmatrix} \rho_1 & 0 \\ 0 & \rho_2 \end{bmatrix} \rightarrow \begin{Bmatrix} v_1(t+T) \\ v_2(t+T) \end{Bmatrix} = \begin{bmatrix} \rho_1 & 0 \\ 0 & \rho_2 \end{bmatrix} \begin{Bmatrix} v_1(t) \\ v_2(t) \end{Bmatrix} \quad (30)$$

- It is easy to notice that, for  $n$  integer

$$v_1(t+T) = \rho_1 v_1(t) \rightarrow v_1(t+nT) = \rho_1^n v_1(t) \quad (31)$$

$$v_2(t+T) = \rho_2 v_2(t) \rightarrow v_2(t+nT) = \rho_2^n v_2(t) \quad (32)$$

- For  $t \rightarrow \infty$  ( $n \rightarrow \infty$ ),  $v_i(t+nT) \rightarrow 0$  if  $|\rho_i| < 1$  and  $v_i(t+nT) \rightarrow \infty$  if  $|\rho_i| > 1$ . **Conclusion: bounded solutions appear if all  $|\rho_i| < 1$ . If at least one  $|\rho_i| > 1$ , unbounded solutions take place.**
- If  $\rho_i = 1$ :  $v_i(t+T) = v_i(t) \rightarrow v_i(t)$  is periodic with period  $T$ ;
- If  $\rho_i = -1$ :  $v_i(t+T) = -v_i(t) \rightarrow v_i(t)$  is periodic with period  $2T$ ;
- Nomenclature:  $\rho_i$  is named Floquet multiplier.

## Case i - $B$ has distinct eigenvalues

- From Eqs. 31 and Eq. 32, we have:

$$v_i(t + T)e^{-\gamma_i(t+T)} = \rho_i e^{-\gamma_i t} e^{-\gamma_i T} v_i(t) \quad (33)$$

- If  $\rho_i = e^{\gamma_i T}$ ,  $v_i(t + T)e^{-\gamma_i(t+T)} = v_i(t)e^{-\gamma_i t}$ . We define  $\phi_i(t) = v_i(t)e^{-\gamma_i t}$ , which is a periodic function of period  $T$  and write the Floquet (or normal) form  $v_i(t) = \phi_i(t)e^{\gamma_i t}$ ;
- Nomenclature:  $\gamma_i$  is the characteristic exponent.

## Case ii - $B$ has equal eigenvalues $\rho_1 = \rho_2 = \rho$

- Case ii-a

$$B = \begin{bmatrix} \rho & 0 \\ 0 & \rho \end{bmatrix} \quad (34)$$

- In the case ii-a, the above discussions still hold;
- Case ii-b

$$B = \begin{bmatrix} \rho & 0 \\ 1 & \rho \end{bmatrix} \quad (35)$$

- In the case ii-b,  $v_1(t+T) = \rho v_1(t)$  and  $v_2(t+T) = v_1(t) + \rho v_2(t)$ . Similarly to already developed,  $v_1(t+T) = \phi_1(t)e^{\gamma t}$ ,  $\rho = e^{\gamma T}$  and  $\phi_1(t) = \phi_1(t+T)$ .
- Using the same approach:

$$\begin{aligned} v_2(t+T)e^{-\gamma(t+T)} &= v_1(t)e^{-\gamma(t+T)} + \rho v_2(t)e^{-\gamma(t+T)} = \\ &= \phi_1(t)e^{-\gamma T} + \rho v_2(t)e^{-\gamma(t+T)} = e^{-\gamma t} v_2(t) + \frac{1}{\rho} \phi_1(t) \end{aligned} \quad (36)$$

## Case ii - $B$ has equal eigenvalues $\rho_1 = \rho_2 = \rho$

- The term  $1/\rho\phi_1(t)$  does not allow writing a normal form like the one written for  $v_1(t)$ . However, as can be seen in Nayfeh (1993), we can write:

$$v_2(t) = e^{\gamma t} \left( \phi_2(t) + \frac{t}{\rho T} \phi_1(t) \right) \quad (37)$$

$\phi_2(t)$  being a periodic function of period  $T$ .

- In the case ii-b, unbounded responses also appear if  $Re\{\gamma\} > 1$ . We use the complex logarithm as follows:

$$\rho = |\rho|e^{i\theta} \rightarrow \ln\rho = \ln(|\rho|e^{i\theta}) = \gamma T \leftrightarrow \ln|\rho| + i\theta = \gamma T \leftrightarrow \frac{\ln|\rho|}{T} + \frac{i\theta}{T} = \gamma \quad (38)$$

- Conclusion:  $Re\{\gamma\} > 0$  if  $|\rho| > 1$ ;
- Note: If  $z = re^{i\theta}$ ,  $r > 0$ ,  $\ln z = \ln r + i\theta$  is one logarithm. We can add an integer number of  $2\pi$  in  $\theta$  to obtain other logarithms.

## How to use?

- We choose a set of fundamental solutions of Eq. 23 satisfying  $u_1(0) = 1, \dot{u}_1(0) = 0, u_2(0) = 0$  and  $\dot{u}_2(0) = 1$ . Using this set into Eqs. 27 and 28, we obtain:

$$\mathbf{A} = \begin{bmatrix} u_1(T) & \dot{u}_1(T) \\ u_2(T) & \dot{u}_2(T) \end{bmatrix} \quad (39)$$

- Floquet multipliers (eigenvalues of  $\mathbf{A}$ ):

$$\begin{aligned} (u_1(T) - \rho)(\dot{u}_2(T) - \rho) - \dot{u}_1(T)u_2(T) &= 0 \leftrightarrow \\ \leftrightarrow \rho^2 - (u_1(T) + \dot{u}_2(T))\rho + \underbrace{(u_1(T)\dot{u}_2(T) - \dot{u}_1(T)u_2(T))}_{\Delta} &= 0 \end{aligned} \quad (40)$$

- $\Delta = \det \mathbf{A}$  is the Wronskian of  $u_1(t)$  and  $u_2(t)$  at  $t = T$ .
- Two solutions of the Hill's equation satisfy:

$$\ddot{u}_1 + p(t)u_1 = 0 \rightarrow u_2\ddot{u}_1 + p(t)u_2u_1 = 0 \quad (41)$$

$$\ddot{u}_2 + p(t)u_2 = 0 \rightarrow u_1\ddot{u}_2 + p(t)u_1u_2 = 0 \quad (42)$$

- From above equations:  $u_1\ddot{u}_2 - u_2\ddot{u}_1 = 0$ .

## How to use?

- If we define  $\Delta(t) = u_1(t)\dot{u}_2(t) - \dot{u}_1(t)u_2(t)$ , we have  $\dot{\Delta}(t) = u_1(t)\ddot{u}_2(t) - \ddot{u}_1(t)u_2(t) = 0$ .
- Conclusion: The Wronskian does not depend on time and  $\Delta(t) = \Delta(0) = 1$ ;
- Substituting this result in Eq. 40, we have

$$\rho^2 - \underbrace{(u_1(T) + \dot{u}_2(T))}_{2\alpha} \rho + 1 = 0 \quad (43)$$

$$\rho_{1,2} = \frac{2\alpha \pm 2\sqrt{\alpha^2 - 1}}{2} = \alpha \pm \sqrt{\alpha^2 - 1} \quad (44)$$

with  $\rho_1\rho_2 = 1$ .

- If  $|\alpha| > 1$ ,  $\rho_1 > 0$  and  $\rho_2 < 0$ , both real-valued. One normal solution is unbounded. **Unstable solutions**;
- If  $|\alpha| < 1$ ,  $\rho_1$  and  $\rho_2$  are complex conjugated with  $|\rho_1| = |\rho_2| = 1$ . Both normal solutions are bounded. **Stable solutions**;
- If  $\alpha = 1$ ,  $\rho_1 = \rho_2 = 1 \rightarrow$  at least one normal solution of period  $T$  appears;
- If  $\alpha = -1$ ,  $\rho_1 = \rho_2 = -1 \rightarrow$  at least one normal solution of period  $2T$  appears;

# How to use?

- 1 We choose a set of parameters of the mathematical model;
- 2 We numerically obtain  $\mathbf{A}$  by integrating the mathematical model using two different pairs of initial conditions. One pair has unitary initial displacement and null initial velocity. The second pair has null initial displacement and unitary velocity;
- 3 For the chosen set of parameters, we compute the eigenvalues of  $\mathbf{A}$  (Floquet multipliers) and we save the one presenting the largest absolute value ( $|\rho^*|$ );
- 4 We change the set of parameters of the mathematical model and repeat steps 2 and 3.
- 5 We plot  $|\rho^*|$  as functions of the parameters of the mathematical model. If  $|\rho^*| > 1$ , we have unbounded responses. On the other hand,  $|\rho^*| < 1$  leads to bounded solutions.

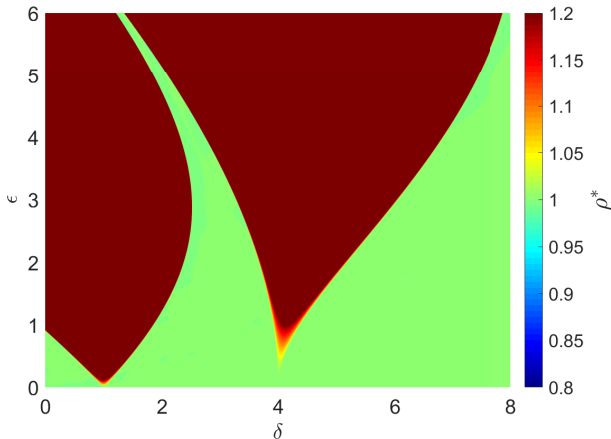


Figure: Stability map.

Using a standard notebook (i7, 10<sup>th</sup> generation, 16Gb RAM), this plot has been obtained in approximately 15 minutes with a  $2,000 \times 2,000$  grid.

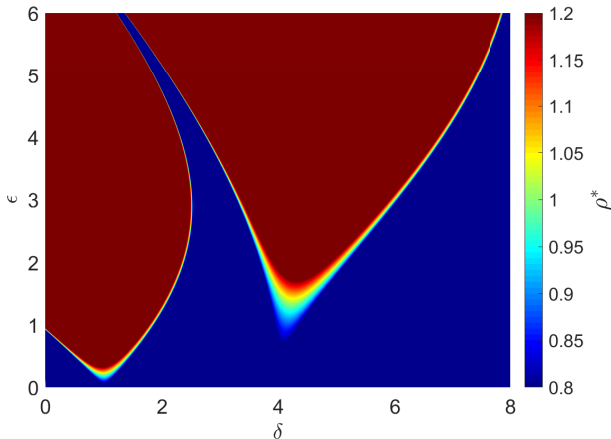


Figure: Stability map.  $\zeta = 0.10$ .

- $\ddot{u} + 2\zeta\dot{u} + (\delta + 2\epsilon \cos 2t)u = 0$
- The increase in the damping shrinks the region of unbounded responses.

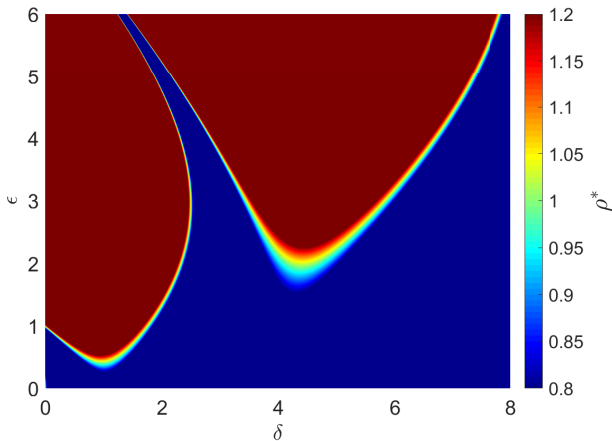


Figure: Stability map.  $\zeta = 0.20$ .



# Outline

- 1 Objectives and references
- 2 General definitions
- 3 Strutt's diagram
- 4 Horizontal cable
- 5 Dynamics of slender and straight offshore structures vertically hanged
- 6 Floquet theory - introduction
- 7 Use of the harmonic balance method (HBM)**

# Use of the harmonic balance method (HBM)

- Focus herein: Obtain the transition curves for the undamped Mathieu's equation  $\ddot{x} + (\delta + 2\epsilon \cos 2\tau)x = 0$ ;
- Notice that the parametric excitation period is  $T = \pi$ ;
- As already discussed, the transition curves are associated with periodic solutions of period  $T$  or  $2T$ .
- We write these solutions in the form of Fourier series, as follows:

$$x(t) = \sum_{n=0}^{\infty} \left( \tilde{a}_n \cos n2\tau + \tilde{b}_n \sin n2\tau \right) + \sum_{n=0}^{\infty} \left( \tilde{c}_n \cos n\tau + \tilde{d}_n \sin n\tau \right) \quad (45)$$

- Notice that the even harmonics (i.e., those with the form  $2n\tau$ ,  $n = 1, 2, \dots$ ) appear in the two sums. Hence, we can write just one sum:

$$x(t) = \sum_{n=0}^{\infty} (a_n \cos n\tau + b_n \sin n\tau) \quad (46)$$

# Use of the harmonic balance method (HBM)

- The following identities are useful:

$$\begin{aligned} \cos 2t \cos n\tau &= \left( \frac{e^{i2\tau} + e^{-i2\tau}}{2} \right) \left( \frac{e^{in\tau} + e^{-in\tau}}{2} \right) = \\ &= \frac{1}{2} \cos((2+n)\tau) + \frac{1}{2} \cos((2-n)\tau) \end{aligned}$$

$$\begin{aligned} \cos 2\tau \sin n\tau &= \left( \frac{e^{i2\tau} + e^{-i2\tau}}{2} \right) \left( \frac{e^{in\tau} - e^{-in\tau}}{2i} \right) = \\ &= \frac{1}{2} \sin((2+n)\tau) + \frac{1}{2} \sin((n-2)\tau) \end{aligned}$$

$\times \cos 2\tau =$

$$= \sum_{n=0}^{\infty} \left[ a_n \left( \frac{\cos((2+n)\tau) + \cos((2-n)\tau)}{2} \right) + b_n \left( \frac{\sin((2+n)\tau) + \sin((n-2)\tau)}{2} \right) \right]$$

$$\ddot{x} = \sum_{n=0}^{\infty} -n^2 (a_n \cos n\tau + b_n \sin n\tau) \quad (47)$$

# Use of the harmonic balance method (HBM)

- Obviously, for the sake of computation, we must choose a number of harmonics to be considered in the expansion.
- Firstly, we consider an expansion considering three harmonics. In this scenario, we have:

$$\begin{aligned}
 \delta x &= \delta a_0 + \delta a_1 \cos \tau + \delta b_1 \sin \tau + \delta a_2 \cos 2\tau + \delta b_2 \sin 2\tau \\
 x \cos 2\tau &= \frac{a_0}{2} (\cos 2\tau + \cos 2\tau) + \frac{a_1}{2} (\cos 3\tau + \cos \tau) + \frac{b_1}{2} (\sin 3\tau - \sin \tau) + \\
 &+ \frac{a_2}{2} (\cos 4\tau + 1) + \frac{b_2}{2} \sin 4\tau \\
 \ddot{x} &= -(a_1 \cos \tau + b_1 \sin \tau + 4a_2 \cos 2\tau + 4b_2 \sin 2\tau)
 \end{aligned} \tag{48}$$

- Substituting Eq. 48 into the Mathieu's equation and collecting the terms of the same trigonometric function (harmonic balance), we obtain:

$$\begin{aligned}
 (-a_1 + \delta a_1 + \epsilon a_1) \cos \tau + (-b_1 + \delta b_1 - \epsilon b_1) \sin \tau + (-4a_2 + \delta a_2 + 2\epsilon a_0) \cos 2\tau + \\
 + (-4b_2 + \delta b_2) \sin 2\tau + (\delta a_0 + \epsilon a_2) + \dots = 0
 \end{aligned} \tag{49}$$

- In the above equation, ... represents harmonic of higher-order, not considered in the expansion.

- Equation 49 can be written in the matrix form as

$$\begin{pmatrix} 0 & -1 + \delta + \epsilon & 0 & 0 & 0 \\ 0 & 0 & -1 + \delta - \epsilon & 0 & 0 \\ 2\epsilon & 0 & 0 & -4 + \delta & 0 \\ 0 & 0 & 0 & 0 & \delta - 4 \\ \delta & 0 & 0 & \epsilon & 0 \end{pmatrix} \begin{Bmatrix} a_0 \\ a_1 \\ b_1 \\ a_2 \\ b_2 \end{Bmatrix} = \begin{Bmatrix} 0 \\ 0 \\ 0 \\ 0 \\ 0 \end{Bmatrix} \quad (50)$$

- Non-trivial solutions exist if

$$\begin{vmatrix} 0 & -1 + \delta + \epsilon & 0 & 0 & 0 \\ 0 & 0 & -1 + \delta - \epsilon & 0 & 0 \\ 2\epsilon & 0 & 0 & -4 + \delta & 0 \\ 0 & 0 & 0 & 0 & \delta - 4 \\ \delta & 0 & 0 & \epsilon & 0 \end{vmatrix} = \\ = (4\delta - \delta^2 + 2\epsilon^2)(-4 + \delta)(-1 + \delta - \epsilon)(-1 + \delta + \epsilon) = 0 \quad (51)$$

- Equation 51 defines an approximation for the transition curves.

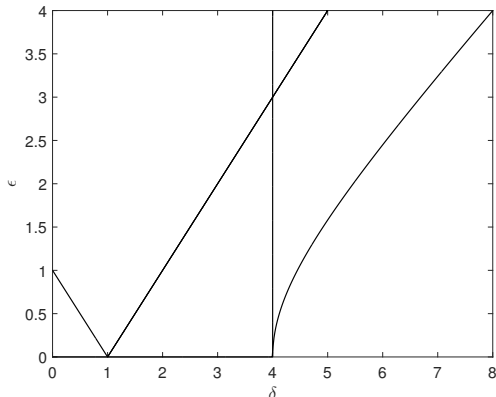


Figure: Extracted from Franzini (2019).

- Points above the transition curves are associated with unbounded solutions;
- If we include more terms in the expansion, the transition curves are better represented. Notice, however, that the mathematical work highly increases and symbolic computation is mandatory.

- This plot has been obtained using seven harmonics in the expansion.

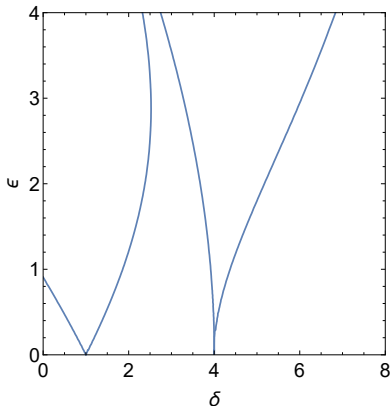


Figure: Extracted from Franzini (2019).

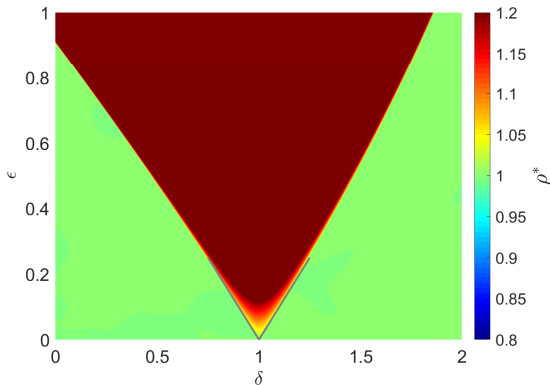


Figure: Stability map. Detail around the principal parametric instability region.  
 $\zeta = 0$ .

- A marked adherence is obtained when comparing the stability map and the transition curves obtained with the HBM using three harmonics (gray curves).

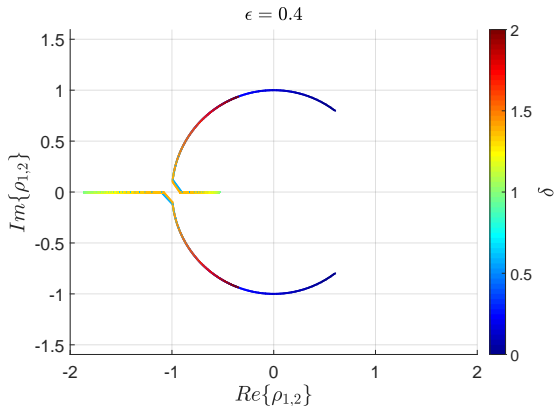


Figure: Floquet multipliers. Detail around the principal parametric instability region.  $\epsilon = 0.4$  and  $\zeta = 0$ .

- Bifurcation occurs when at least one Floquet multiplier crosses the circumference of radius 1. Particularly, if the crossing is through  $-1$ , we have a period-doubling bifurcation.

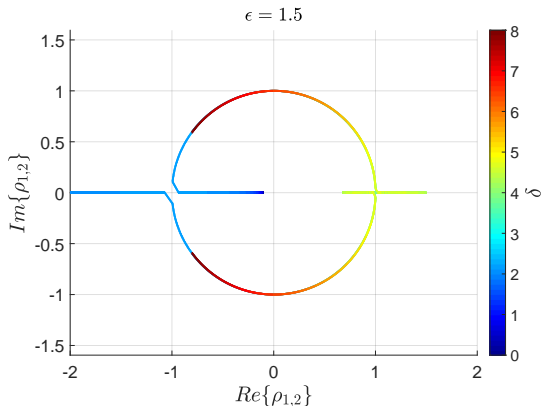


Figure: Floquet multipliers.  $\epsilon = 1.5$  and  $\zeta = 0$ .

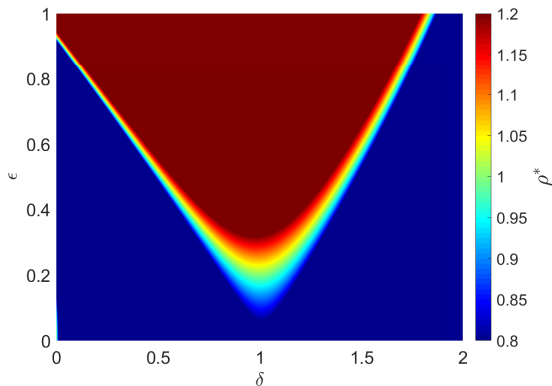


Figure: Stability map. Detail around the principal parametric instability region.  
 $\zeta = 0.10$ .

# Floquet multipliers: $\zeta = 0.10$

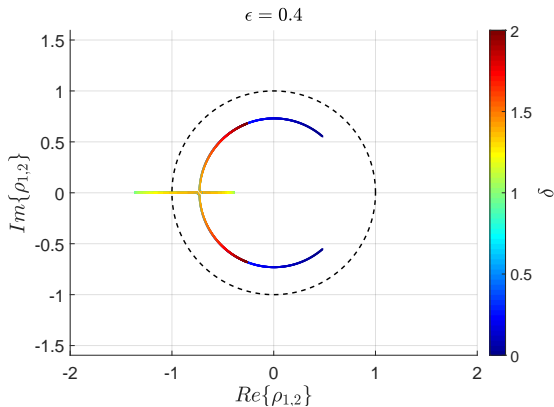


Figure: Floquet multipliers. Detail around the principal parametric instability region.  $\epsilon = 0.4$  and  $\zeta = 0.10$ .

- For certain values of  $\delta$ , there are Floquet multipliers inside the circumference of radius 1.